ARTICLE

Nanostructured VO_2 Photocatalysts for Hydrogen Production

Yuquan Wang,[†] Zhengjun Zhang,[†,*] Yu Zhu,[†] Zhengcao Li,[†] Robert Vajtai,[‡] Lijie Ci,[‡,§] and Pulickel Madhavapanicker Ajayan[‡,§]

[†]Advanced Materials Laboratory, Department of Materials Science and Engineering, Tsinghua University, Beijing 100084, P.R. China, and [‡]Nanotechnology Center, Rensselaer Polytechnic Institute, Troy, New York 12180. [§]Present Address: Mechanical Engineering and Materials Science Department, Rice University, Houston, Texas 77005.

ABSTRACT Vanadium dioxide (VO_2) is a well-known semiconductor material with a band gap of 0.7 eV, and is seldom used as a photocatalyst. We report here a new crystal structure for nanostructured VO_2, with body-centered-cubic (bcc) structure and a large optical band gap of ~2.7 eV, which surprisingly shows excellent photocatalytic activity in hydrogen production. The bcc VO_2 phase exhibited a high quantum efficiency of ~38.7% when synthesized as nanorods. Using films of the aligned VO_2 nanorods, the hydrogen production rate can be tuned by varying the incident angle of UV light on the films and reaches a high rate of 800 mmol/m^2/h from a mixture of water and ethanol under UV light, at a power density of ~27 mW/cm^2, allowing possible commercial application of this material as photoassisted hydrogen generators.

KEYWORDS: vanadium oxide · nanorod · photocatalysis · hydrogen generator

As a clean and renewable energy source, hydrogen production *via* photoelectrolysis has stimulated great research interest from 1972.[1–3] Since water and light are naturally abundant, the photoassisted water splitting procedure has been considered an economic route to generate hydrogen.[4,5] One promising method of this route is the light-induced photooxidation of water, where metal oxides are often employed as the photocatalyst.[6] For example, TiO_2 has been proven an effective catalyst for hydrogen production from water−methanol solutions,[7] for example, TiO_2 thin films prepared by sol−gel processes induced a hydrogen evolution rate of ~0.7 mmol/m^2/h from water cleavage.[8] However, the efficiency of these catalysts needs to be further improved for commercial applications of hydrogen generators.[5,6] It is thus of great significance to develop new catalyst materials with desired surface morphology to increase the efficiency of photoassisted hydrogen generators.

Vanadium oxides in the V_2O_5−V_2O_3 system are complex and many intermediate oxide phases exist within this compositional range.[9,10] Among them VO_2 is an interesting narrow band gap (*i.e.*, 0.7 eV) semiconductor, which changes reversibly from a monoclinic to a tetragonal structure at ~68 °C, leading to correspondingly a semiconductor-to-metal transition.[11] This makes VO_2 a promising candidate material for applications in fast switching, electrochromic, and other applications.[10] However, due to its narrow band gap, VO_2 has never been considered as a candidate material for photocatalytic production of hydrogen. Since V_2O_5 has been widely used as catalysts in industries, it is of interest to investigate the possibility that VO_2 crystallizes into other forms which exhibit excellent photocatalytic activity, especially when synthesized into nanostructures.

Vanadium oxides can be prepared by a variety of synthetic approaches.[12–15] We employed here a thermal oxidation approach to deposit nanostructures of vanadium oxide on silicon substrate, which is capable of producing large-scale arrays of aligned nanorods and other nanostructures of metal oxides at relatively low substrate temperatures.[16,17] With this technique large-scale arrays of aligned VO_2 nanorods were deposited on silicon substrates.

We report here the observation of a new structure (*i.e.*, bcc) for VO_2 when synthesized as nanorods and the investigation on the electrical and optical properties. Interestingly, owing to its large optical band gap, the newly observed bcc VO_2 phase exhibited excellent photocatalytic activity with a quantum efficiency of 38.7%. This makes it a promising photocatalyst candidate for applications in hydrogen generators.

RESULTS AND DISCUSSIONS

Figure 1 panels a−c show scanning electron microscopy (SEM) images of the vana-

*Address correspondence to zjzhang@tsinghua.edu.cn.

Received for review April 16, 2008 and accepted June 18, 2008.

Published online July 1, 2008.
10.1021/nn800223s CCC: $40.75

dium oxide nanostructures deposited on the substrate at the previously mentioned conditions, taken with a JEOL JSM-6301 SEM working at 20 kV. Figure 1d shows a bright-field transmission electron microscopy (TEM) image of the rods with the inset showing the corresponding selected area electron diffraction (SAD) pattern; both were taken with a JEOL JEM-2010 TEM working at 200 kV. One sees that the rods are ~6 μm long, several hundred nm in diameter, and are single crystalline. It is also noticed that the rods are of sharp conical shapes and are vertically aligned. X-ray diffraction (XRD) analysis of these aligned rods was performed by a Rigaku X-ray diffractometer using the Cu Kα radiation, by the θ−2θ coupled scan and the small-angle diffraction, respectively. The patterns obtained by the θ−2θ coupled scan and the small angle diffraction indicate that the rods are strongly textured as they grow on the silicon substrate, yet they could not match any known oxides of vanadium. Therefore, it is very difficult to get the structure information of the rods from the XRD patterns. Since the rods are single-crystalline, we tried to identify their structure *via* SAD analysis with a JEOL JEM-2010 TEM working at 200 kV. To determine the structure, we performed SAD analysis for more than twenty rods. For each rod, three SAD patterns were taken along different axes and were indexed. All indexing results indicated that the rods have a bcc structure with a lattice constant of ~0.94 nm. Figure 2 panels a−c show a typical set of the SAD patterns, taken from one rod at a tilt angle of 0°, 11°, and 18°, respectively. The indexing results suggest that the incident electron beam was along the [001], [$\bar{1}$50], and [$\bar{1}$30] directions, respectively. Figure 2d shows a HRTEM image corresponding to Figure 2a, the inset of which is anenlarged part of the image. It is seen that the rod has a sharp tip of ~15 nm size and that the rod is grown along the <002> direction which is in agreement with the SAD analysis. Using this lattice structure, the XRD pattern (see Supporting Information) can also be well indexed.

The composition of these cone-shaped rods was measured by electron energy loss spectrometry (EELS). Figure 3 a is a typical EELS spectrum of the rods, showing signals of oxygen and vanadium signals. The spectrum gave an estimation of the atomic ratio of oxygen/vanadium very close to 2.0. We have done EELS analysis for a large number of rods, and in all cases a ratio of ~2.0 was obtained. Rutherford backscattering spectrometer (RBS) analysis using a 1.7 MeV He^+ beam (see Supporting Information) also gave an overall composition close to VO_2. It is thus concluded that the cone-shaped rods deposited on the silicon substrate are bcc VO_2. The formation of the VO_2 nanorods was due to the fast evaporation and oxidation of vanadium atoms in the rough vacuum and deposition on the substrate at relatively low temperatures. Similar growth behavior was also observed for other metal oxides by this approach.[16,17]

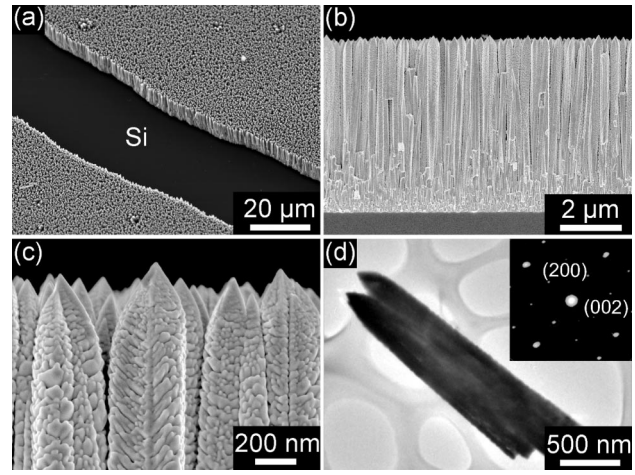

Figure 1. SEM images of the cone-shaped vanadium oxides rods formed on Si substrates: (a) a low-magnification image, (b) a side-view image, and (c) a top-view SEM image; (d) TEM image of the rods, showing clearly the sharp tip; inset shows a corresponding SAD pattern of the rod.

The electrical and optical properties of this bcc VO_2 phase are very different from the known VO_2 phases.[10,11] Figure 3b shows the electrical resistance (R) of the bcc VO_2 film at elevated temperature; inset plots R in the logarithm scale *versus* the reverse of the temperature ($1/T$). For comparison, the electrical resistance of a monoclinic VO_2 thin film (prepared by magnet sputtering) is shown in Figure 3c. One notices that both films are semiconducting, however, the monoclinic VO_2 underwent a first order phase transition at ~68 °C (*i.e.*, from monoclinic to tetragonal structure) resulting in a big jump in R,[10,11] while the bcc VO_2 exhibited a second-order phase transition around 120 °C. By fitting the inset with two straight lines using the Arrhenius equation of $R = R_0 \exp(-E_a/kT)$, the activation energy (E_a) was estimated to be ~0.103 and ~0.267 eV, at temperatures below and above 120 °C, respectively. Figure 3d shows the reflectance spectrum of the VO_2 film as measured in the UV−visible range; the inset shows how to estimate the optical band gap from the spectrum. By fitting the absorption edge of the spec-

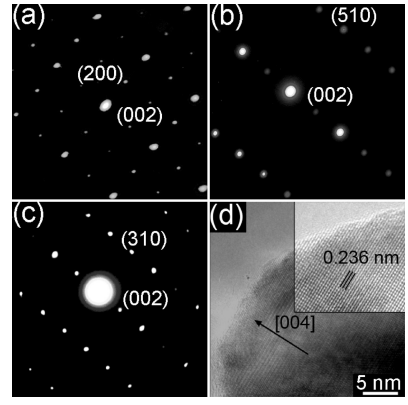

Figure 2. SAD patterns of a bcc VO_2 rod obtained with the incident electron beam along directions of (a) [010], (b) [$\bar{1}$50], and (c) [$\bar{1}$30], respectively; (d) HRTEM image corresponding to Figure 2a.

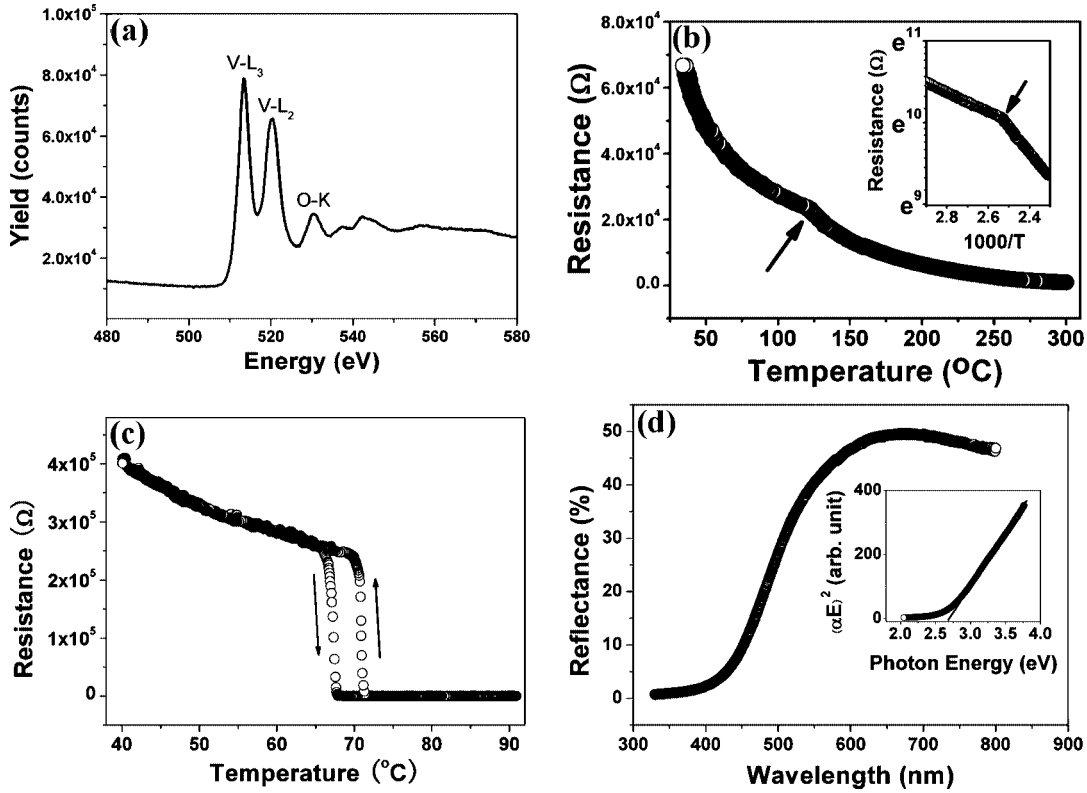

Figure 3. The (a) EELS spectrum and (b) the electrical resistance of the bcc VO_2 rods versus the temperature, inset of which is a logarithm plot; (c) the electrical resistance of a thin film of the monoclinic VO_2 phase; and (d) the reflectance spectrum of the bcc VO_2 film in the UV−visible range, inset of which shows how to derive the optical band gap from the absorption edge.

trum using the Tauc relationship, the optical band gap of the bcc VO_2 was estimated to be 2.7 eV, which is much larger than the value of 0.7 eV reported for the monoclinic VO_2.[11] These results confirm that the bcc VO_2 phase, different from the well-known monoclinic and tetragonal phases, is a new phase in the vanadium oxide family.

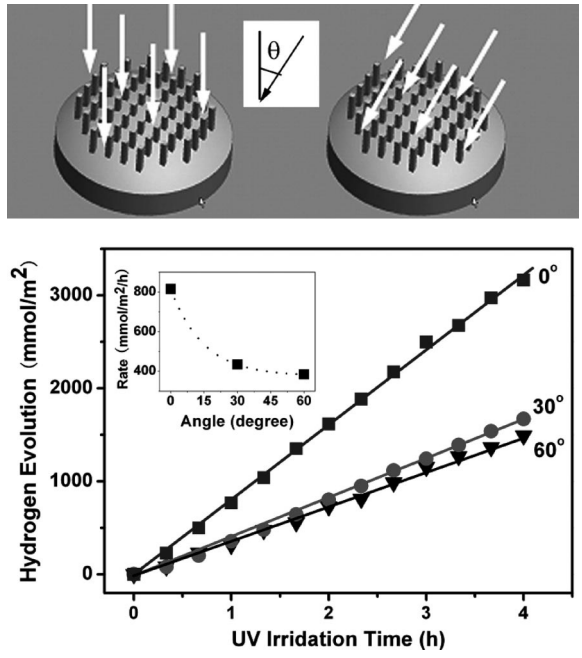

Figure 4. Hydrogen evolution from a solution of water and ethanol (5:1 ratio) catalyzed by the VO_2-nanostructured films. Inset shows the dependence of the hydrogen production rate on the incident angle of the light.

Because of the relatively large optical band gap, that is, 2.7 eV and the porous morphology shown by Figure 1c, the bcc VO_2 rods might be applied as a photocatalyst for hydrogen production through water splitting. Figure 4 shows hydrogen evolution from a mixture of ethanol and water with a ratio of 1:5, under a mercury lamp at 500 W. The inset of the figure shows the dependence of the hydrogen production rate as a function of the incident angle of the light. The silicon substrate contribution to the hydrogen generation was removed by measuring the hydrogen evolution at same conditions using a silicon reference of a same size. It is noticed that for three different incident angles, the hydrogen production was linearly increased with the expose time. Within 4 h, no saturation or degradation was observed. When the light was incident along the axis of the rods, the hydrogen production rate reached a maximum of ~800 mmol/m^2/h. To calculate the quantum efficiency of the bcc VO_2 film, the power density of the light illuminating on the film was measured using a radiometer. By counting the number of photons with energy >2.7 eV (the optical band gap of the bcc VO_2) from the spectrum of the mercury light, the quantum

efficiency was calculated to be ~38.7%. This high value is probably due to the band structure of the bcc VO_2 and the porous surface morphology of the rods.

Another interesting point is that the hydrogen production rate is very dependent on the incident angle of the light illuminating on the film. One sees that when the light was incident normally on the sample, that is, along the axis of the rods, the hydrogen production rate reached the maximum. If the light was incident off the axis of the rods, the hydrogen production got decreased. For example, the hydrogen production rate decreased almost half when the light was 30° off the axis of the rods. This is due to the vertical alignment of the rods, as less amount of light was absorbed by the film to enable the photoreaction when the light was incident off the axis of the rods. With this feature one might adjust the hydrogen production rate by controlling the incident angle of the light on the film.

The efficiency of the catalyst in hydrogen production through water splitting is a key factor that influences the commercialization of this technique. Metal oxides powders, for example, TiO_2,[7,18–20] $KNbO_x$,[6] CoO_x,[21] WO_x,[22] $LaMnO_x$,[23] and FeO_x[24] *etc.*, are reported to be of good catalytic efficiency. In solutions of distilled water and ethanol as we used here, they exhibited a catalytic hydrogen generation rate of 0.5−2 mmol/g/h.[21] Through further treatments, for example, doping with La or Mn or coating with Pt, Au, or Ni and by adjusting the pH value of the solutions by adding some salts (like Na_2S), the catalytic efficiency has been enhanced. The best efficiency achieved till now is for Pt-coated TiO_2, with which hydrogen could be generated at a rate of ~5 mmol/g/h in MeOH.[19] In recent years, thin film catalysts have also attracted attention.[8,25–28] For example, with TiO_2 thin films in solutions of distilled water and methanol hydrogen could be generated at a rate of ~0.7 mmol/m^2/h.[8,18,25–28] Similarly, modifying the surface of the films and adjusting the pH value of the solutions could further enhance the efficiency. For instance, in coating the films with novel metals such as Pt, TiO_2 thin films reached a rate of ~50 mmol/m^2/h in 0.1 M Na_2S aqueous solution and Pt-coated CdS films reached a rate of ~100 mmol/m^2/h.[26] Since the quantum efficiency of our bcc VO_2 films is ~38.7%, the hydrogen generation rate achieved here is about 800 mmol/m^2/h, which might enable the commercialization of photoassisted hydrogen generators.

CONCLUSIONS

In summary, we observed that VO_2 could crystallize into a bcc structure when it was synthesized as nanorods. Different from the known monoclinic and tetragonal structures the bcc VO_2 phase has an optical band gap of 2.7 eV and exhibited a second-order phase transition at ~120 °C. Besides, unlike the nonphotocatalytic monoclinic and tetragonal VO_2 phases, the bcc VO_2 exhibited excellent photocatalytic activity, that is, with a quantum efficiency of 38.7%, in hydrogen generation by photoassisted water splitting. With this catalyst a hydrogen production rate of ~800 mmol/m^2/h was achieved under a 500 W mercury light.

MATERIALS AND METHODS

Si (001) wafers were supersonically cleaned in acetone, alcohol, and deionized water baths and placed ~4 cm below a sheet of vanadium (99.99%, 5 mm × 50 mm × 0.7 mm) connected to two copper electrodes in a vacuum chamber. The chamber was pumped to ~5 Pa and then a voltage of ~2 V was applied to the two electrodes, resulting in a current of ~65 A passing through the vanadium sheet which heats the sheet to ~900 °C rapidly, leading to the deposition of nanostructures on the silicon substrate. During deposition the substrate temperature was <350 °C.

After deposition, the morphology, the structure, and the composition of the deposits were examined by SEM, TEM, SAD, XRD, EELS, RBS, and ultraviolet photoelectron spectrometer, respectively. The electrical and optical properties of the deposits were also measured.

The photocatalytic property of the vanadium oxide nanostructures was evaluated by measuring the hydrogen evolution from a mixture of water and ethanol under UV light at room temperature. The hydrogen production experiment was carried out in a quartz reactor cooled by running water, and the entire system was hermetically sealed. The catalyst film (with a size of 5 mm × 5 mm) was placed at the bottom of the quartz reactor, filled with 20 mL of ethanol and 100 mL of water. To remove the air in the system, nitrogen flux was introduced into the system for 30 min before the experiment. In the experiment a 500 W mercury lamp was used as the UV light source to offer photons, where the power density of UV light radiated on the catalyst film was measured to be 270 W/m^2 by a radiometer. The hydrogen evolution upon UV light radiation was measured every 20 min with a Shimadzu GC-14B gas chromatography system.

Acknowledgment. The authors are grateful to the financial support by the National Natural Science Foundation of China (Grants 10675070, 10575061), and the National Basic Research Program of China (973 program, 2007CB936601). P.M.A. and R.V. thank the Rensselaer Nanotechnology Center for support.

Supporting Information Available: Additional composition analysis and structure characterization data. This material is available free of charge *via* the Internet at http://pubs.acs.org.

REFERENCES AND NOTES

1. Fujishima, A.; Honda, K. Electrochemical Photolysis of Water at a Semiconductor Electrode. *Nature* **1972**, *238*, 37–38.
2. Turner, J. A. A Realizable Renewable Energy Future. *Science* **1999**, *285*, 687–689.
3. Tryk, D. A.; Fujishima, A.; Honda, K. Recent Topics in Photoelectrochemistry: Achievements and Future Prospects. *Electrochim. Acta* **2000**, *45*, 2363–2376.
4. Bolton, J. R. The Photochemical Conversion and Storage of Solar Energy: An Historical Perspective. *Sol. Energy Mater. Sol. Cells* **1995**, *38*, 543–554.
5. Kang, Z. C.; Wang, Z. L. Novel Oxides for Cycled Hydrogen Production from Methane and Water Using a Temperature Swing. *Adv. Mater.* **2003**, *15*, 521–526.
6. Takata, T.; Tanaka, A.; Hara, M.; Kondo, J. N.; Domen, K. Recent Progress of Photocatalysts for Overall Water Splitting. *Catal. Today.* **1998**, *44*, 17–26.

7. Bamwenda, G. R.; Tsubota, S.; Nakamura, T.; Haruta, M. Photoassisted Hydrogen Production from a Water-Ethanol Solution: A Comparison of Activities of Au-TiO_2 and Pt-TiO_2. *J. Photochem. Photobio. A: Chem.* **1995**, *89*, 177–189.
8. Shangguan, W. F.; Yoshida, A.; Chen, M. X. Physicochemical Properties and Photocatalytic Hydrogen Evolution of TiO_2 Films Prepared by Sol-Gel Processes. *Sol. Energy Mater. Sol. Cells* **2003**, *80*, 433–441.
9. Adler, D. Mechanisms for Metal-Nonmetal Transitions in Transition-Metal Oxides and Sulfides. *Rev. Mod. Phys.* **1968**, *40*, 714–736.
10. Heckingbottom, R.; Linnett, J. W. Structure of Vanadium Dioxide. *Nature* **1962**, *194*, 678.
11. Thomas, G. A.; Rapkine, D. H.; Carter, S. A.; Millis, A. J.; Rosenbaum, T. F.; Metcalf, P.; Honig, J. M. Observation of the Gap and Kinetic Energy in a Correlated insulator. *Phys. Rev. Lett.* **1994**, *73*, 1529–1532.
12. Nishio, S.; Kakahana, M. Evidence for Visible Light Photochromism of V_2O_5. *Chem. Mater.* **2002**, *14*, 3730–3733.
13. Bay, N. T. B.; Tien, P. M.; Badilescu, S.; Djaoued, Y.; Bader, G.; Girouard, F. E.; Truong, V.; Nguyen, L. Optical and Electrochemical Properties of Vanadium Pentoxide Gel Thin Films. *J. Appl. Phys.* **1996**, *80*, 7041–7045.
14. Barreca, D.; Armelao, L.; Caccavale, F.; Noto, V. D.; Gregori, A.; Rizzi, G. A.; Tondello, E. Highly Oriented V_2O_5 Nanocrystalline Thin Films by Plasma-Enhanced Chemical Vapor Deposition. *Chem. Mater.* **2000**, *12*, 98–103.
15. Talledo, A.; Granqvist, C. G. Electrochromic Vanadium-Pentoxide-Based Films: Structural, Electrochemical, and Optical Properties. *J. Appl. Phys.* **1995**, *77*, 4655–4666.
16. Liu, J. G.; Zhao, Y.; Zhang, Z. J. Low-Temperature Synthesis of Large-Scale Arrays of Aligned Tungsten Oxide Nanorods. *J. Phys. Condens. Mater.* **2003**, *15*, L453–L461.
17. Zhang, Z. J.; Zhao, Y.; Zhu, M. M. NiO Films Consisting of Vertically Aligned Cone-Shaped NiO Rods. *Appl. Phys. Lett.* **2006**, *88*, 033101.
18. Matsuoka, M.; Kitano, M.; Takeuchi, M.; Tsujimaru, K.; Anpo, M.; Thomas, J. M. Photocatalysis for New Energy Production Recent Advances in Photocatalytic Water Splitting Reactions for Hydrogen Production. *Catal. Today.* **2007**, *122*, 51–61.
19. Herrmann, J. M. From Catalysis by Metals to Bifunctional Photocatalysis. *Top. Catal.* **2006**, *39*, 1–2.
20. Ikeda, M.; Kusumoto, Y.; Somekawa, S.; Ngweniform, P.; Ahmmad, B. Effect of Graphite Silica on TiO_2 Photocatalysis in Hydrogen Production From Water-Methanol Solution. *J. Photochem. Photobiol., A* **2006**, *184*, 306–312.
21. Qin, Y.; Wang, G.; Wang, Y. Study on the Photocatalytic Property of La-Doped CoO/$SrTiO_3$ for Water Decomposition to Hydrogen. *Catal. Commun.* **2007**, *8*, 926–930.
22. Hameed, A.; Gondal, M. A.; Yamani, Z. H. Effect of Transition Metal Doping on Photocatalytic Activity of WO_3 for Water Splitting under Laser Illumination: Role of 3d-Orbitals. *Catal. Commun.* **2004**, *5*, 715–719.
23. Kida, T.; Guan, G.; Yamada, N. Hydrogen Production from Sewage Sludge Solubilized in Hot-Compressed Water Using Photocatalyst under Light Irradiation. *Int. J. Hydrogen Energy* **2004**, *29*, 269–274.
24. Gondal, M. A.; Hameed, A.; Yamani, Z. H.; Suwaiyan, A. Production of Hydrogen and Oxygen by Water Splitting Using Laser Induced Photo-Catalysis over Fe_2O_3. *Appl. Catal., A* **2004**, *268*, 159–167.
25. Cui, W. Q.; Feng, L. R.; Xu, C. H.; Lü, S. J.; Qiu, F. L. Hydrogen Production by Photocatalytic Decomposition of Methanol Gas on Pt/TiO_2 Nano-Film. *Catal. Commun.* **2004**, *5*, 533–536.
26. So, W. W.; Kim, K. J.; Moon, S. J. Photo-Production of Hydrogen over the CdS-TiO_2 Nano-Composite Particulate Films Treated with $TiCl_4$. *Int. J. Hydrogen Energy* **2004**, *29*, 229–234.
27. Ni, M.; Leung, M.; Leung, D.; Sumathy, K. A Review and Recent Developments in Photocatalytic Water-Splitting Using TiO_2 for Hydrogen Production. *Renewable Sustainable Energy Rev.* **2007**, *11*, 401–425.
28. Sreethawong, T.; Puangpetch, T.; Chavadej, S.; Yoshikawa, S. Quantifying Influence of Operational Parameters on Photocatalytic H_2 Evolution over Pt-Loaded Nanocrystalline Mesoporous TiO_2 Prepared by Single-Step Sol-Gel Process with Surfactant Template. *J. Power Sources* **2007**, *165*, 861–869.